CHEMISTRY
A EUROPEAN JOURNAL

DOI: 10.1002/chem.200601074

Coordination of Triply Charged Lanthanum in the Gas Phase: Theory and Experiment

Tujin Shi, Alan C. Hopkinson, and K. W. Michael Siu*[a]

Abstract: Ion–molecule reactions between complexes $[La(CH_3CN)_n]^{3+}$ (n=6–9) or $[La(NC(CH_2)_4CN)_n]^{3+}$ (n=3–4) and water were studied at low collision energies in the second quadrupole of a tandem mass spectrometer. The products $[La(CH_3CN)_p(H_2O)_{8-p}]^{3+}$ (p=6–8) and $[La(NC(CH_2)_4CN)_q(H_2O)_{8-2q}]^{3+}$ (q=3–4) had the highest relative abundances. This strongly suggests that the preferred coordination number of La^{3+} is eight. Similarly, the coordination number of Ca^{2+} was reexamined both experimentally and theoretically, and was found to be six, in good agreement with previous observations. Density functional calculations provide strong evidence that the primary solvation shell of $[La(L)_n]^{3+}$ consists of eight ligands; additional ligands reside in a second solvation shell and are hydrogen bonded to one or two water molecules in the first shell.

Keywords: density functional calculations · ion–molecule reactions · lanthanum · mass spectrometry · solvent effects

Introduction

Ion solvation has fascinated chemists for many years.[1] Investigations of ion solvation have provided a wealth of information on ion–solvent and ion–ligand interactions,[2,3] both of which are of importance not only to gas-phase ion chemistry, but also to solution chemistry.[4–6] A combination of ESI-MS and high-level quantum chemical theory can be used to study ion solvation in the gas phase systematically.[7–13] Such studies can provide details of the first and second solvation shells around metal ions and metal–ligand binding in complexes, and also enhance our understanding of the underlying structural chemistries in these metal-containing systems.

The advent of ESI has broadened the study of metal-ion solvation by facilitating the generation of doubly and even triply charged ion–solvent complexes in the gas phase.[7,8,14–17] The solvation of alkaline-earth-metal ions has been investigated extensively by both experiment[7,8] and theory.[10–13] For the dications of Mg, Ca, and Sr, the first six ligands constitute the first solvation shell, and additional molecules are accommodated in the second shell. The sequential binding energies, however, indicate crowding in the first shell of Mg complexes.[7a] This has been proven by experiments on $[Mg(H_2O)_6]^{2+}$ that show six water molecules located in the first solvation shell at low temperatures, whereas, at higher temperatures, the most likely structure has four water molecules in the first and two water molecules in the second solvation shell.[8c] There are no gas-phase experimental data for Be available to confirm a preference for tetrahedral geometry; however, theoretical data indicate that the most stable configuration of the $[Be(H_2O)_6]^{2+}$ complex corresponds to a 4+2 arrangement of the ligands.[18] Studies on the fragmentations of $[Mn(H_2O)_n]^{2+}$ and $[Mn(ROH)_n]^{2+}$ (in which ROH is methanol, ethanol, 1-propanol, or 2-propanol), in combination with theoretical calculations, indicate that the preferred structures are $[Mn(H_2O)_4]^{2+}\cdot(n-4)H_2O$ and $[Mn(ROH)_4]^{2+}\cdot(n-4)H_2O$; the first solvation shells have tetrahedral geometries, with the additional solvent molecules in the second shells hydrogen bonded to those in the first shells.[19]

Solvent coordination of trivalent metal ions in the gas phase has not yet been examined in detail; only the observations and fragmentations of solvated trivalent metal-ion complexes have been reported. Most solvents examined to date are aprotic: these include acetonitrile,[15b,16c,20] dimethyl

---

[a] Dr. T. Shi, Prof. A. C. Hopkinson, Prof. K. W. M. Siu
Department of Chemistry and Centre for
Research in Mass Spectrometry, York University
4700 Keele Street, Toronto, Ontario, M3J 1P3 (Canada)
Fax: (+1) 416-736-5939
E-mail: kwmsiu@yorku.ca

Supporting information for this article is available on the WWW under http://www.chemeurj.org/ or from the author. This includes information on low-energy collisions between Ca^{2+}–acetonitrile complexes and water molecules; binding energies of $[Ca(HCN)_2(H_2O)_m]^{2+}$ complexes; first-shell versus second-shell coordination in $[Ca(HCN)_2(H_2O)_m]^{2+}$ complexes.

sulfoxide (DMSO),[14a,15b,16b] dimethyl formamide,[14a] and acetone,[15b,20] with the lone protic solvent being diacetone alcohol (4-hydroxy-4-methyl-2-pentanone).[16a] Despite sustained efforts with water and a number of alcohols, no M^{3+} complexes with any protic ligand (P) have been produced until very recently.[21] Even in this work, the M^{3+} requires a minimum of ≈16 water molecules to preserve vitality.[21] Typically, charge-reduced species are observed, produced by interligand proton transfer within the complex and yielding mainly $[M(P-H)(P)_n]^{2+}$ and $[MX(P)_n]^{2+}$, in which X is the counteranion of the metal salt.[14a,15b,17c,20] This tendency to charge reduction is believed to be driven mainly by the large third ionization energies (IEs) of M. Of all the trivalent metals, La has the smallest third IE at 19.2 eV.[22] The electronic configuration of lanthanum is [Xe]$5d^16s^2$; consequently, La^{3+} has a closed electronic shell.

In ESI-MS, the relative abundances of the solvated complexes can be fine-tuned by changing the collision energy. In MS scans, the extent of fragmentation and ion–molecule reactions is a function of the collision energy in the sampling (lens) region. Under MS/MS conditions, this is also dependent on the collision energy; a second variable is the pressure of the neutral collision partner. (Depending on the reaction, there may be conditions under which neither energy nor pressure is a particularly sensitive parameter. These are conditions best-suited to analytical purposes.) If the pressure of the collision gas is kept constant, energy-resolved collision-induced dissociation (CID) curves, plots of relative ion abundance versus collision energy, can be obtained.[23–26] Under single-collision conditions, threshold dissociation energies can be determined after kinetic shifts are taken into account.[25–26] These results, coupled with computed potential-energy diagrams, are frequently used to shed light on the fragmentation chemistries of the precursor ions. A second type of investigation involves examination of ion–molecule equilibria attained in the ion source/lens region by means of low-energy collisions, for example, those between doubly charged metal ions and water.[7a]

Under low-energy ("mild") collision conditions, it is our observation that the preferred coordination number of metal ions can be determined. Here, we report the observation and examination of the $[La(CH_3CN)_n(H_2O)_m]^{3+}$ complexes in the gas phase. The water molecules bind to $[La(CH_3CN)_n]^{3+}$ complexes to preferentially complete the first solvation shell. Acetonitrile is a polar molecule with a high dipole moment (3.92 D), and, hence, forms tightly bound complexes held together by a strong charge–dipole interaction.[27] Binding occurs through one site, the nitrogen atom. Also, as a result of the linear arrangement of the heavy atoms in acetonitrile (C_{3v} symmetry), the steric hindrance between ligated acetonitriles is small. Thus, acetonitrile is an almost ideal small ligand for exploring the solvent coordination of trivalent metal ions. In this investigation, we have studied systematically the solvation chemistry of La^{3+} by both experiment and theory, and have also attempted to determine the preferred coordination number of La^{3+} in the gas phase. To verify the validity of our method, we have also re-examined the coordination number of Ca^{2+}, previously shown to be six, by means of the mixed complexes, $[Ca(CH_3CN)_n(H_2O)_m]^{2+}$.

Experimental Section

Mass spectrometry: Experiments were performed by using two prototypes of the API 3000 triple-quadrupole mass spectrometer and the QSTAR, a hybrid quadrupole/time-of-flight (TOF) mass spectrometer (both Applied Biosystems/MDS SCIEX). Samples were 100 μM lanthanum(III) nitrate in acetonitrile or hexanedinitrile. Confirmatory experiments were performed with solutions in [D$_3$]acetonitrile. The samples were introduced into the pneumatically assisted ESI source at a flow rate of 3 μL min^{-1}. The lens voltages were optimized to produce abundant $[La(CH_3CN)_n]^{3+}$ ($n=3$–10) and $[La(NC(CH_2)_4CN)_m]^{3+}$ ($m=2$–5) ions. All chemicals and solvents were from Sigma–Aldrich (St. Louis, MO). MS/MS experiments were performed by mass-selecting the precursor ions with the first quadrupole, colliding them with a mixture of water and nitrogen in the second quadrupole, and mass-analyzing the resulting products with the third quadrupole or TOF analyzer. The water/nitrogen mixture was boiled off from liquid nitrogen, which contained water as a minor component.[28,29] The pressure of the water/nitrogen mixture was varied to adjust and probe the extent of hydration in the products.

Computational methods: Geometry optimizations and energy calculations were performed with Gaussian 98[30] by using the B3LYP exchange-correlation functional.[31–33] The sdd relativistic effective core potential (ECP)[34] and basis set was used for calcium. The Stuttgart–Dresden ECP along with a (7s6p5d2f)/[5s4p3d2f] basis set[35] for the valence and outermost core (5s5p) electrons was used for lanthanum. This latter basis set was obtained by partially uncontracting the (7s6p5d)/[5s4p3d] basis associated with the ECP and adding two uncontracted f functions (energy-optimized exponents $\alpha=0.85$, 0.35).[35] For convenience, we simply refer to this ECP and basis set as sdd-f. The 6-31G(d) doubly split-valence basis set augmented with the set of polarization functions on heavy atoms was used for C, N, and O atoms and the 31G basis set was used for the H atom. Because of the relatively large size of $[La(CH_3CN)_6(H_2O)_m]^{3+}$ ($m=1$–4), for reasons of tractability, all calculations were performed on $[La(HCN)_6(H_2O)_m]^{3+}$ as a model of the former. All stationary points were characterized by harmonic vibrational frequency calculations, and all energies include zero-point vibrational-energy corrections. Inclusion of diffuse and polarization functions on oxygen has been shown to improve the binding energies[12] and consequently, single-point energies were calculated for the $[La(HCN)_6(H_2O)_m]^{3+}$ system at B3LYP/sdd-f/6-31+G(d,p)//B3LYP/sdd-f/6-31G(d) with zero-point energy corrections (using a scaling factor of 0.9804[36]). Relative enthalpies are reported at 0 K and relative free energies at 298 K.

Results and Discussion

$[Ca(CH_3CN)_n(H_2O)_m]^{2+}$ and $[Ca(HCN)_n(H_2O)_m]^{2+}$ complexes: Experimental examinations of $[Ca(CH_3CN)_n(H_2O)_m]^{2+}$ as well as calculations of $[Ca(HCN)_n(H_2O)_m]^{2+}$ complexes revealed that Ca^{2+} binds up to six ligands in its first solvation shell with additional ligands in a second shell, in accordance with literature data.[7a,12] This proves that our methods for examining metal-ion solvation are effective and should provide reliable information on the solvation of La^{3+}. For the sake of brevity, details of the Ca^{2+} results are not detailed here, but are available as Supporting Information.

Low-energy collisions between La^{3+}–acetonitrile complexes and water molecules: The spectra of $[La(CH_3CN)_n]^{3+}$ were obtained with a variety of laboratory collision energies (E_{lab}) and collision gas pressures. In general, as the pressure increases under low collision-energy conditions, $[\mathrm{La}(\mathrm{CH_3CN})_n]^{3+}$ tends to associate increasingly with water molecules. Figure 1 shows adducts with $n=6$, 7, and 8 and Figure 2 shows the variation in abundance of some of these products with respect to the collision gas pressure.

A careful examination of the collision-activated chemistries reveals the following reaction channels:

a) Ligand loss

$$[\mathrm{La}(\mathrm{CH_3CN})_n]^{3+} \rightarrow [\mathrm{La}(\mathrm{CH_3CN})_m]^{3+} + (n-m)\mathrm{CH_3CN} \tag{1}$$

b) Water attachment

$$[\mathrm{La}(\mathrm{CH_3CN})_n]^{3+} + m\mathrm{H_2O} \rightarrow [\mathrm{La}(\mathrm{CH_3CN})_n(\mathrm{H_2O})_m]^{3+} \tag{2}$$

c) Ligand exchange and water attachment

$$\begin{aligned}&[\mathrm{La}(\mathrm{CH_3CN})_n]^{3+} + q\mathrm{H_2O} \rightarrow \\ &[\mathrm{La}(\mathrm{CH_3CN})_{n-q}(\mathrm{H_2O})_q]^{3+} + q\mathrm{CH_3CN}\end{aligned} \tag{3}$$

d) Ligand exchange, proton transfer, and water attachment

$$\begin{aligned}&[\mathrm{La}(\mathrm{CH_3CN})_n]^{3+} + m\mathrm{H_2O} \rightarrow \\ &[\mathrm{La}(\mathrm{OH})(\mathrm{CH_3CN})_{n-p}(\mathrm{H_2O})_{m-q-1}]^{2+} + [(\mathrm{CH_3CN})_p(\mathrm{H_2O})_q\mathrm{H}]^{+}\end{aligned} \tag{4}$$

Notably, after ion–molecule reactions of ions $[\mathrm{La}(\mathrm{CH_3CN})_n]^{3+}$, the most abundant complexes were invariably $[\mathrm{La}(\mathrm{CH_3CN})_n(\mathrm{H_2O})_m]^{3+}$ for which $n+m=8$: $[\mathrm{La}(\mathrm{CH_3CN})_6(\mathrm{H_2O})_2]^{3+}$ (Figure 1a), $[\mathrm{La}(\mathrm{CH_3CN})_7(\mathrm{H_2O})]^{3+}$ (Figure 1b), and $[\mathrm{La}(\mathrm{CH_3CN})_8]^{3+}$ and $[\mathrm{La}(\mathrm{CH_3CN})_7(\mathrm{H_2O})]^{3+}$ (Figure 1c). By contrast, reactions of $[\mathrm{La}(\mathrm{CD_3CN})_9]^{3+}$ resulted in only low-abundance complexes containing nine ligands with high-abundance complexes of $[\mathrm{La}(\mathrm{CD_3CN})_8]^{3+}$ and $[\mathrm{La}(\mathrm{CD_3CN})_7(\mathrm{H_2O})]^{3+}$ (Figure 1d). In the CID of $[\mathrm{La}(\mathrm{CH_3CN})_8]^{3+}$, the abundance of the parent ion remains high, there is very little addition of water, and exchange of one $\mathrm{CH_3CN}$ for $\mathrm{H_2O}$ is the dominant reaction. Figure 2 supports the conclusion that the most abundant $[\mathrm{La}(\mathrm{CH_3CN})_n(\mathrm{H_2O})_m]^{3+}$ complexes are those in which $n+m=8$. At q2 pressures below 6 mTorr, increasing the pressure (increasing the abundance of water) leads to an almost linear decrease in the relative abundances of $[\mathrm{La}(\mathrm{CH_3CN})_n]^{3+}$ and an almost linear increase in those of $[\mathrm{La}(\mathrm{CH_3CN})_n(\mathrm{H_2O})_m]^{3+}$. At pressures above 6 mTorr, the changes are much less pro-

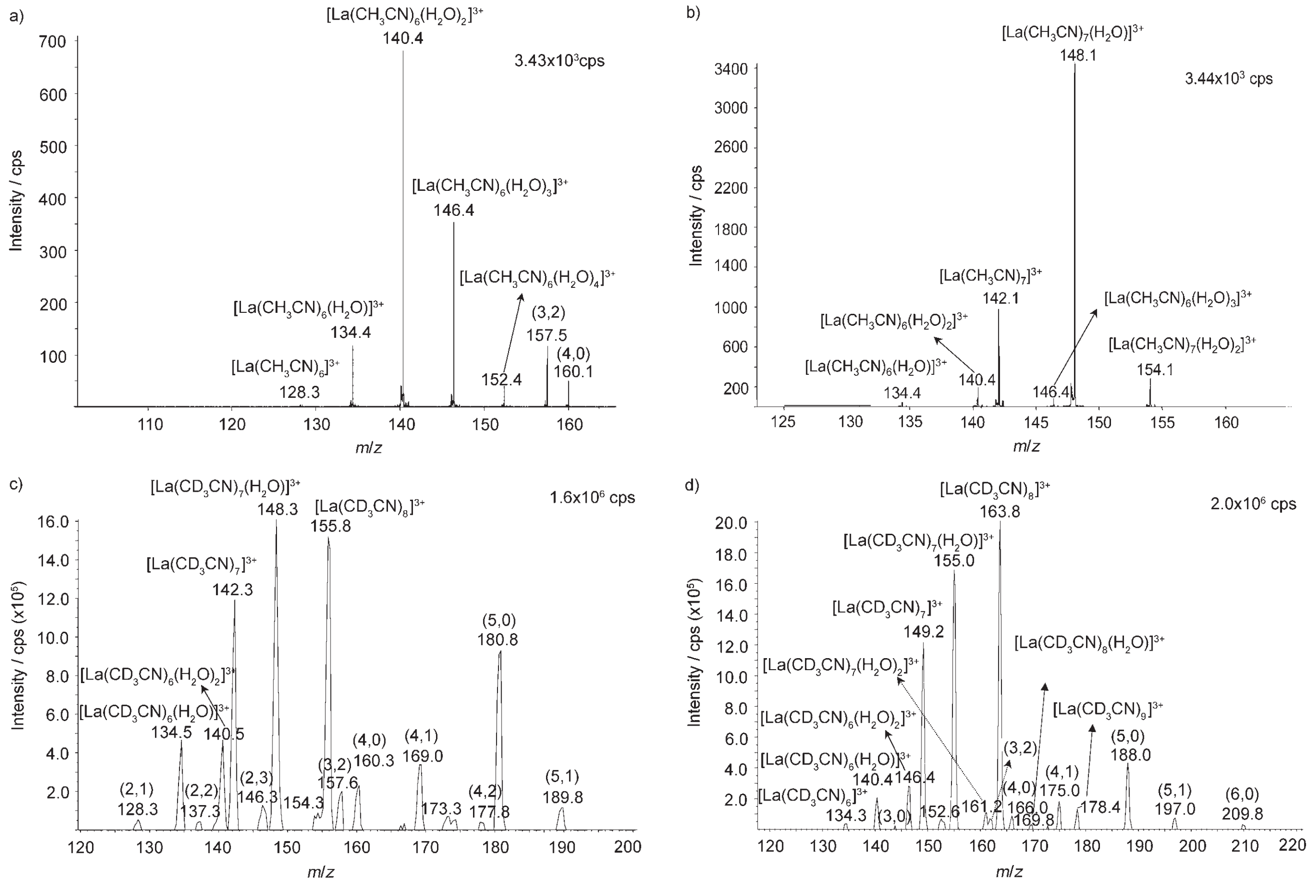

Figure 1. Collisional activation of a) $[\mathrm{La}(\mathrm{CH_3CN})_6]^{3+}$, b) $[\mathrm{La}(\mathrm{CH_3CN})_7]^{3+}$ recorded with the Centaur, a hybrid quadrupole/TOF mass spectrometer; c) $[\mathrm{La}(\mathrm{CH_3CN})_8]^{3+}$, d) $[\mathrm{La}(\mathrm{CD_3CN})_9]^{3+}$ recorded with the API 3000 triple-quadrupole mass spectrometer: laboratory collision energy, 15 eV; collision gas pressure, 8 mTorr. Peaks labeled with numbers (n,m) represent dications $[\mathrm{LaOH}(\mathrm{CH_3CN},\mathrm{CD_3CN})_n(\mathrm{H_2O})_m]^{2+}$.

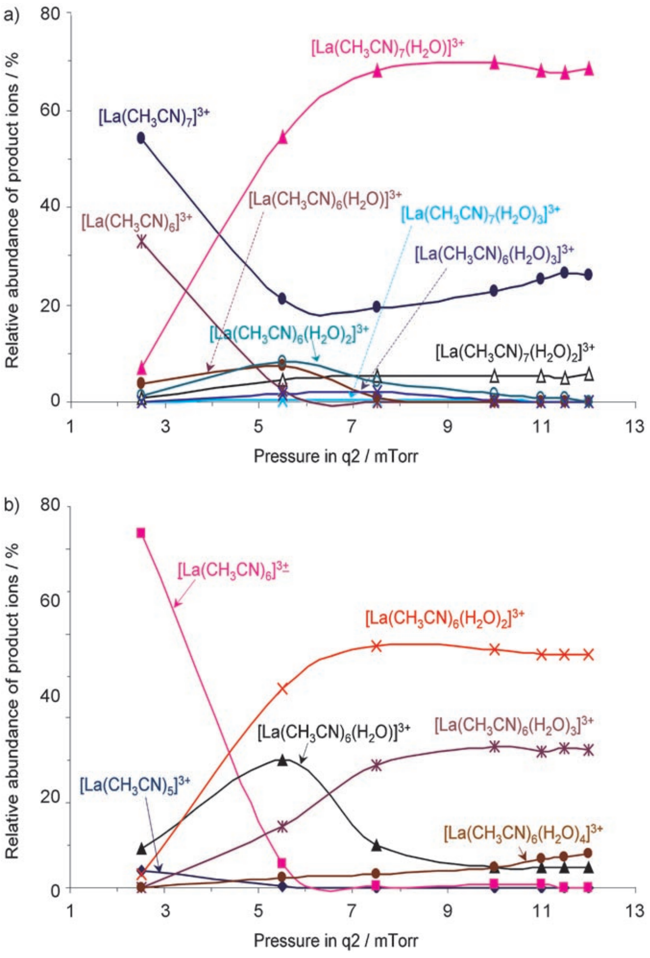

Figure 2. Relative abundance of product ions versus collision gas pressure, $E_{lab} = 6$ eV. Precursor ion: a) $[La(CH_3CN)_7]^{3+}$ and b) $[La(CH_3CN)_6]^{3+}$.

nounced and level off at 10 mTorr. On the basis of this evidence, we conclude that La^{3+} binds preferentially and strongly eight ligands, and binds a ninth one more weakly.

These results are consistent with the interpretation that the first eight ligated solvent molecules reside in the first solvation shell of La^{3+} with additional molecules being accommodated in an outer shell. The facile elimination of acetonitrile from $[La(CH_3CN)_9]^{3+}$ and $[La(CD_3CN)_9]^{3+}$ at relatively low collision energies indicates that the ninth ligand is only weakly bound and strongly suggests that adducts with more than eight CH_3CN are best described as $[La(CH_3CN)_8]^{3+} \cdot m CH_3CN$. If n is 6 or 7, water molecules may either add or replace the acetonitrile molecules to occupy the primary solvation shell, until the eighth ligand is attached. Additional water molecules may reside only in an outer solvation shell and bind to the solvent molecules in the inner shell by means of hydrogen bonds to create the ions $[La(CH_3CN)_{8-m}(H_2O)_m]^{3+} \cdot (n+m-8)(H_2O)$.

Low-energy collisions between La^{3+}–hexanedinitrile complexes and water molecules: Hexanedinitrile, $NC(CH_2)_4CN$, is a bidentate aprotic ligand. Electrospraying hexanedinitrile solutions of La^{3+} produces complexes $[La(NC(CH_2)_4CN)_n]^{3+}$, in which n is typically 2–4. Figure 3a,b shows products of the ion–molecule reactions for $[La(NC(CH_2)_4CN)_n]^{3+}$, in which $n = 3$ and 4. Whereas $[La(NC(CH_2)_4CN)_3]^{3+}$ tends to associate with two water molecules to form $[La(NC(CH_2)_4CN)_3(H_2O)_2]^{3+}$ (Figure 3a), [La(NC-

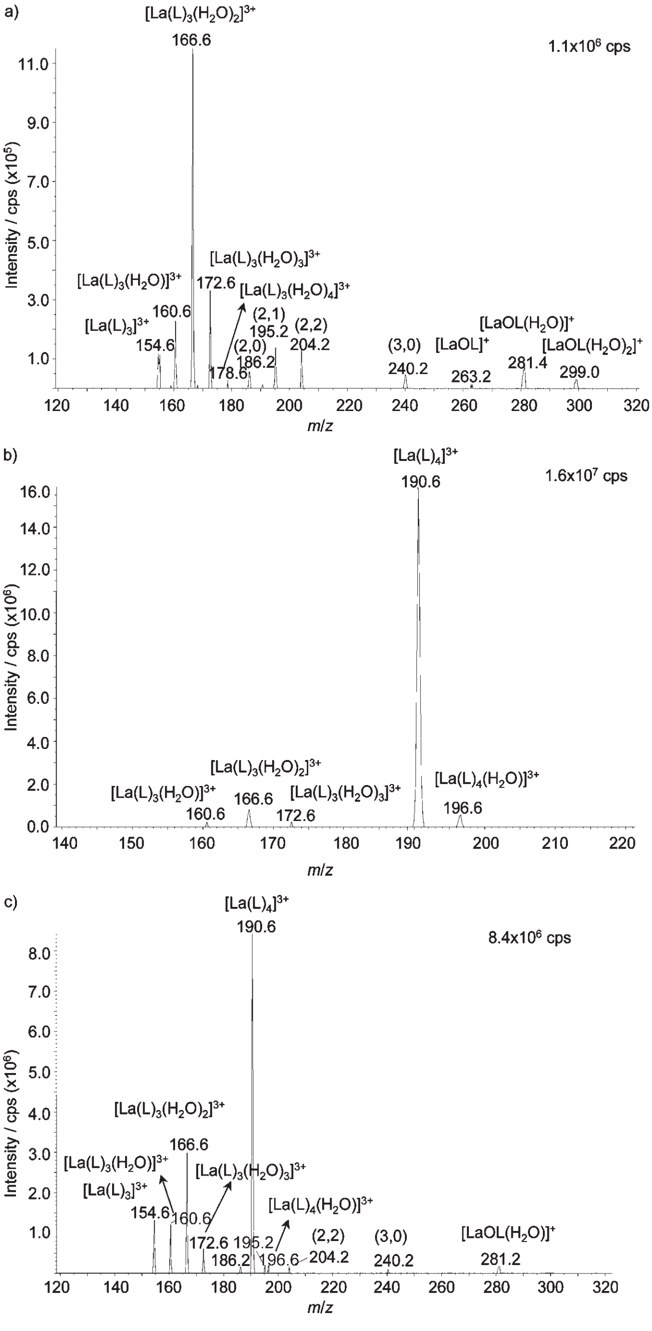

Figure 3. Spectra recorded by using the API 3000 triple-quadrupole mass spectrometer. Collisional activation of a) $[La(NC(CH_2)_4CN)_3]^{3+}$ (at $E_{lab} = 15$ eV), b) $[La(NC(CH_2)_4CN)_4]^{3+}$ (at $E_{lab} = 15$ eV), and c) $[La(NC(CH_2)_4CN)_4]^{3+}$ (at $E_{lab} = 30$ eV) by colliding with wet nitrogen gas ($P = 1.0$ mTorr). L represents a $NC(CH_2)_4CN$ ligand; peaks labeled with numbers (n,m) represent dications $[LaOH(NC(CH_2)_4CN)_n(H_2O)_m]^{2+}$.

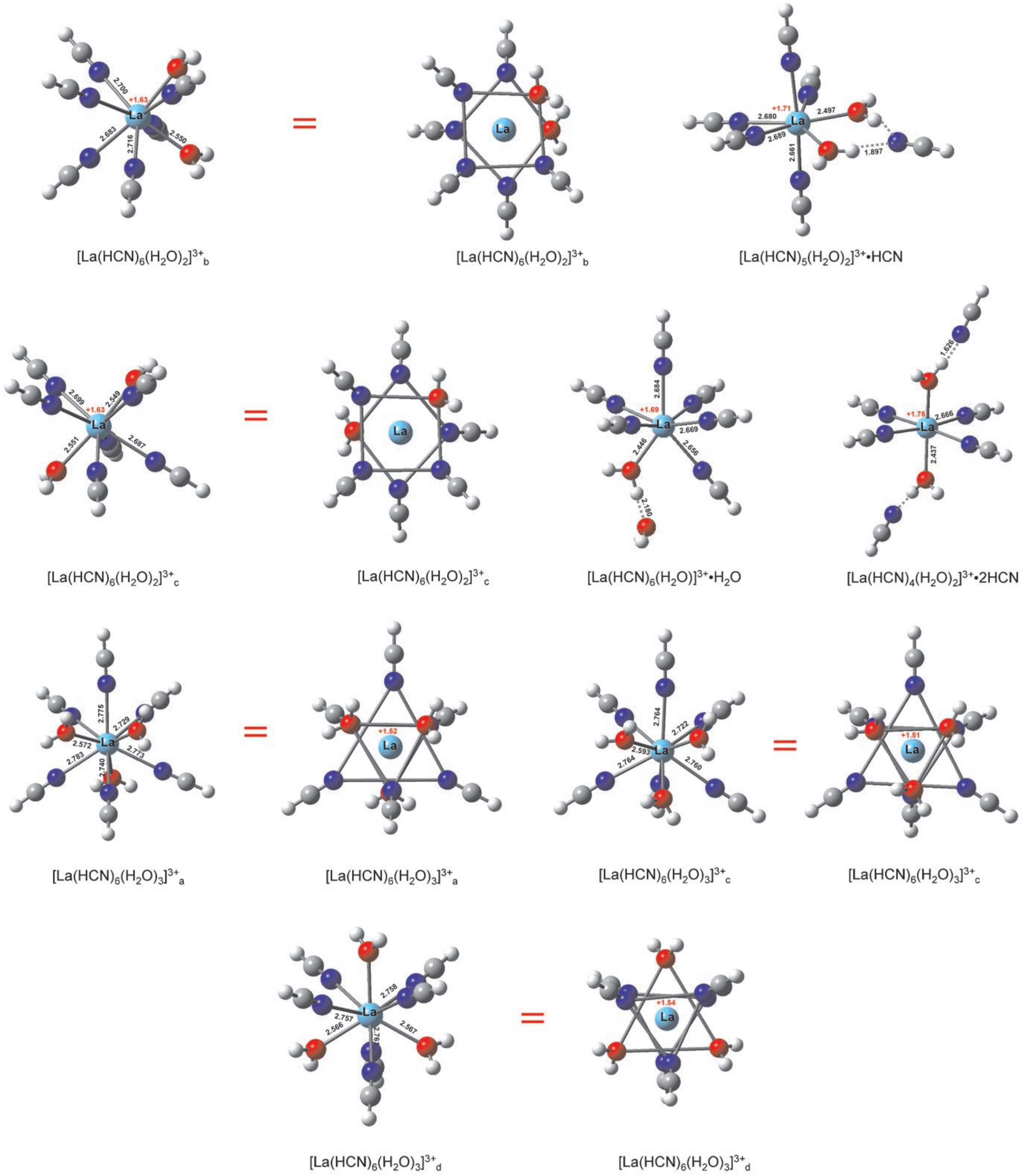

$[La(HCN)_6(H_2O)_2]^{3+}{}_b$ $[La(HCN)_6(H_2O)_2]^{3+}{}_b$ $[La(HCN)_5(H_2O)_2]^{3+}\bullet HCN$

$[La(HCN)_6(H_2O)_2]^{3+}{}_c$ $[La(HCN)_6(H_2O)_2]^{3+}{}_c$ $[La(HCN)_6(H_2O)]^{3+}\bullet H_2O$ $[La(HCN)_4(H_2O)_2]^{3+}\bullet 2HCN$

$[La(HCN)_6(H_2O)_3]^{3+}{}_a$ $[La(HCN)_6(H_2O)_3]^{3+}{}_a$ $[La(HCN)_6(H_2O)_3]^{3+}{}_c$ $[La(HCN)_6(H_2O)_3]^{3+}{}_c$

$[La(HCN)_6(H_2O)_3]^{3+}{}_d$ $[La(HCN)_6(H_2O)_3]^{3+}{}_d$

Figure 4. Selected lower-energy structures of $[La(HCN)_6(H_2O)_m]^{3+}$ ($m = 1$–4). Bond lengths and Mulliken charges (electron units), calculated at the B3LYP/sdd-f/6-31G(d) level, are shown.

$(CH_2)_4CN)_4]^{3+}$ is quite unreactive. The latter appears to be able to accommodate only one additional water molecule, but in only low abundance (Figure 3b). Even after doubling the collision energy (from 15 to 30 eV), $[La(NC(CH_2)_4CN)_4]^{3+}$ remains the most abundant ion (Figure 3c). At this higher collision energy, the loss of one ligand is observed and the product, $[La(NC(CH_2)_4CN)_3]^{3+}$, further associates with up to three water molecules; again, the eight-co-

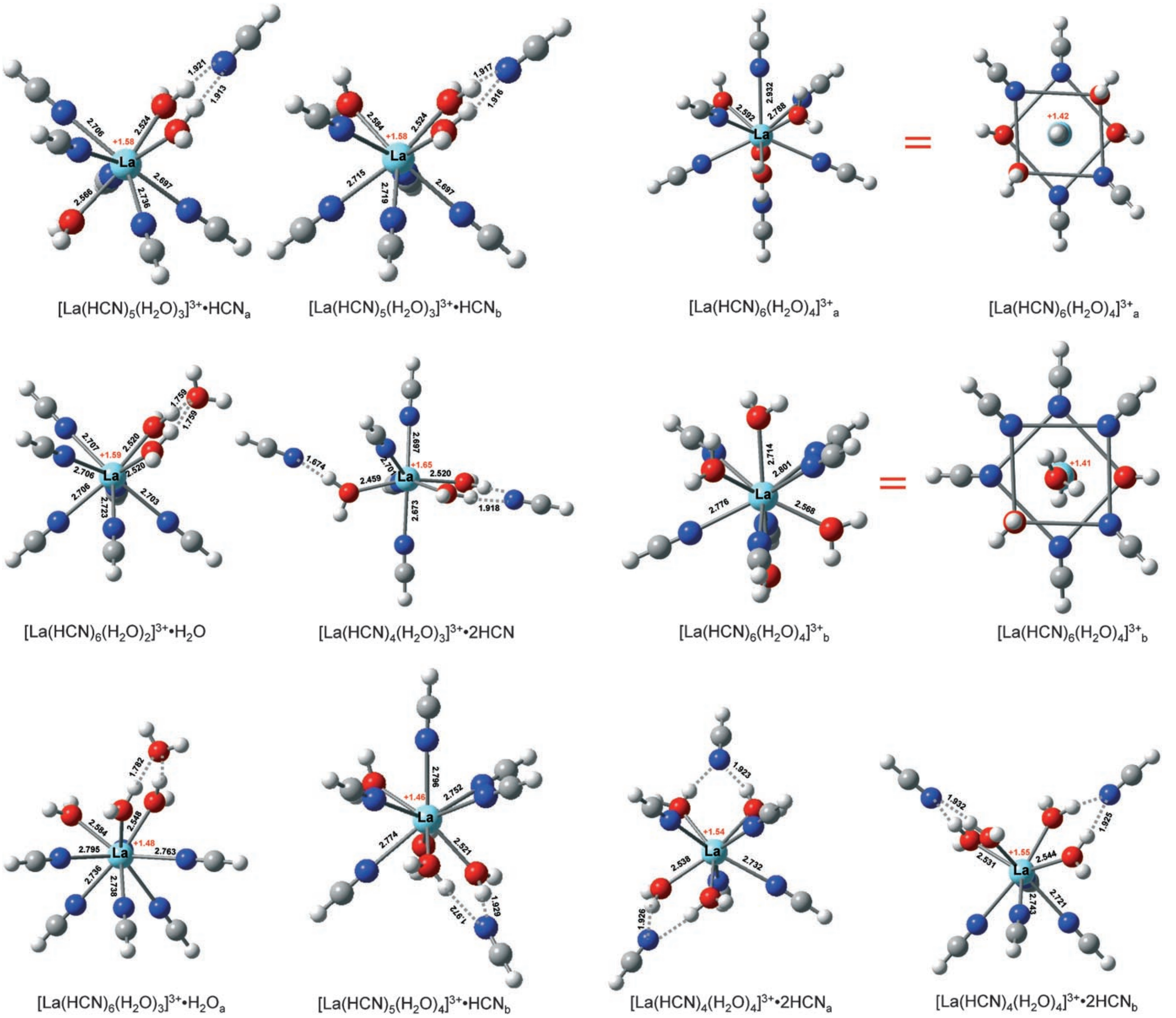

$[La(HCN)_5(H_2O)_3]^{3+}\cdot HCN_a$ $[La(HCN)_5(H_2O)_3]^{3+}\cdot HCN_b$ $[La(HCN)_6(H_2O)_4]^{3+}{}_a$ $[La(HCN)_6(H_2O)_4]^{3+}{}_a$

$[La(HCN)_6(H_2O)_2]^{3+}\cdot H_2O$ $[La(HCN)_4(H_2O)_3]^{3+}\cdot 2HCN$ $[La(HCN)_6(H_2O)_4]^{3+}{}_b$ $[La(HCN)_6(H_2O)_4]^{3+}{}_b$

$[La(HCN)_6(H_2O)_3]^{3+}\cdot H_2O_a$ $[La(HCN)_5(H_2O)_4]^{3+}\cdot HCN_b$ $[La(HCN)_4(H_2O)_4]^{3+}\cdot 2HCN_a$ $[La(HCN)_4(H_2O)_4]^{3+}\cdot 2HCN_b$

Figure 4. Continued

ordinate complex, $[La(NC(CH_2)_4CN)_3(H_2O)_2]^{3+}$, has the highest abundance among the complexes of $[La(NC(CH_2)_4CN)_3(H_2O)_n]^{3+}$.

All the above experiments indicate that La^{3+} binds preferentially eight ligands in the gas phase, that is, complexes of the form $[La(L)_8]^{3+}$ appear to be more stable than complexes with coordination numbers 6, 7, and 9. These results were reproducible in many series of experiments spanning several months and were obtained by using two different instruments (a triple-quadrupole and a hybrid quadrupole/TOF mass spectrometer).

Theoretical studies: Geometry optimizations were performed on complexes $[La(HCN)_6(H_2O)_m]^{3+}$ (m=1–4). HCN is a good model for CH_3CN because the metal is bound to the nitrile group. Replacement of CH_3 by H reduces the size of the ligand and eliminates rotation of the methyl group, thus facilitating geometric optimizations. Many possible isomers were considered and calculated. The lower-energy structures are shown in Figure 4. Total electronic energies, including zero-point energies (E), total binding energies (E_{BE}), sequential binding energies (ΔH^o_0), and sequential free energies (ΔG^o_{298}) for the complexes $[La(HCN)_6(H_2O)_m]^{3+}$ (m=1–4) are given in Table 1. E_{BE}, ΔH^o_0, and ΔG^o_{298} are defined as follows:

$$E_{BE} = E(La^{3+}) + nE(L) - E[La(L)_n]^{3+} \tag{5}$$

$$\Delta H^o_{0(n-1,n)} = E[La(L)_{n-1}]^{3+} + E(L) - E[La(L)_n]^{3+} \tag{6}$$

$$\Delta G^o_{298(n-1,n)} = G[La(L)_{n-1}]^{3+} + G(L) - G[La(L)_n]^{3+} \tag{7}$$

in which L=HCN or H_2O. The lowest-energy structures identified by these calculations are used as the basis for the

Table 1. Total electronic energies (E) [Hartree], including zero-point energy, total binding energies (E_{BE}) [kcal mol^{-1}], sequential binding energies (ΔH^o_0) [kcal mol^{-1}], and sequential free energies (ΔG^o_{298}) [kcal mol^{-1}] according to Equations (5)–(7) calculated at the B3LYP level for complexes $[La(HCN)_n(H_2O)_m]^{3+}$ ($n=1$–6, $m=1$–4).

Complex	$E^{[a]}$	$E^{[b]}$	$E_{BE}^{[a]}$	$E_{BE}^{[b]}$	$\Delta H^{o[a]}_0$	$\Delta H^{o[b]}_0$	$\Delta G^{o}_{298}{}^{[a]}$
$[La(HCN)]^{3+}$	–123.49714	–123.50045	112.3	109.3	112.3	109.3	105.5
$[La(HCN)_2]^{3+}$	–217.04430	–217.05141	200.8	194.9	88.5	85.7	81.3
$[La(HCN)_3]^{3+}$	–310.56831	–310.57927	274.7	266.1	73.9	71.2	65.2
$[La(HCN)_4]^{3+}$	–404.07566	–404.09063	338.2	326.9	63.5	60.8	54.9
$[La(HCN)_5]^{3+}$	–497.55789	–497.57678	385.9	371.9	47.7	45.0	39.5
$[La(HCN)_6]^{3+}$	–591.03024	–591.05292	427.4	410.6	41.5	38.7	34.0
$[La(HCN)_6(H_2O)]^{3+}$	–667.47440	–667.51181	462.8	439.3	35.4	28.7	25.5
$[La(HCN)_6(H_2O)_2]^{3+}{}_b$	–743.91178	–743.96428	493.9	464.0	31.1	24.7	21.0
$[La(HCN)_6(H_2O)_2]^{3+}{}_c$	–743.91172	–743.96429	493.9	464.0	31.1	24.7	21.5
$[La(HCN)_6(H_2O)]^{3+}\cdot H_2O$	–743.90477	–743.96099	489.5	461.9	26.7	22.6	18.8
$[La(HCN)_5(H_2O)_2]^{3+}\cdot HCN$	–743.90883	–743.96190	492.0	462.5	29.2	23.2	19.9
$[La(HCN)_4(H_2O)_2]^{3+}\cdot 2\,HCN$	–743.89610	–743.95178	484.1	456.2	21.3	16.8	14.1
$[La(HCN)_6(H_2O)_3]^{3+}{}_a$	–820.33974	–820.40786	519.1	483.1	25.2	19.1	15.2
$[La(HCN)_6(H_2O)_3]^{3+}{}_c$	–820.33891	–820.40747	518.6	482.9	24.7	18.9	14.5
$[La(HCN)_6(H_2O)_3]^{3+}{}_d$	–820.33906	–820.40776	518.7	483.1	24.8	19.0	14.7
$[La(HCN)_5(H_2O)_3]^{3+}\cdot HCN_a$	–820.34384	–820.41228	521.6	485.9	27.8	21.9	19.0
$[La(HCN)_5(H_2O)_3]^{3+}\cdot HCN_b$	–820.34409	–820.41248	521.8	486.0	28.0	22.0	18.9
$[La(HCN)_6(H_2O)_2]^{3+}\cdot H_2O$	–820.34623	–820.41551	523.2	487.9	29.3	23.9	19.0
$[La(HCN)_4(H_2O)_3]^{3+}\cdot 2\,HCN$	–820.33771	–820.40748	517.8	482.9	24.0	18.9	16.0
$[La(HCN)_6(H_2O)_4]^{3+}{}_a$	–896.75758	–896.84084	538.0	495.6	18.9	12.5	9.3
$[La(HCN)_6(H_2O)_4]^{3+}{}_b$	–896.756244	–896.84036	537.1	495.3	18.0	12.2	7.6
$[La(HCN)_6(H_2O)_3]^{3+}\cdot H_2O_a$	–896.76977	–896.85487	545.6	504.4	26.5	21.3	15.2
$[La(HCN)_5(H_2O)_4]^{3+}\cdot HCN_b$	–896.76994	–896.85518	545.7	504.6	26.6	21.5	15.1
$[La(HCN)_4(H_2O)_4]^{3+}\cdot 2\,HCN_a$	–896.77341	–896.85787	547.9	506.3	28.8	23.1	20.6
$[La(HCN)_4(H_2O)_4]^{3+}\cdot 2\,HCN_b$	–896.77473	–896.85937	548.7	507.2	29.6	24.1	20.0

[a] Calculated at the B3LYP/sdd-f/6-31G(d) level. [b] Calculated at the B3LYP/sdd-f/6-31+G(d,p)//B3LYP/sdd-f/6-31G(d) level with scaled ZPE. The coordinates are available upon request.

discussion on ligand coordination. In Table 1, to indicate complex structures, ligands placed within square brackets are in the first solvation shell, and those preceded by a dot (•) are in the second shell. In the text, the former is used to indicate the general formula as well as structural information. Ambiguity is avoided because, whenever structural information is intended, it will be clear from the adjacent text.

Structures of complexes $[La(HCN)_6(H_2O)_m]^{3+}$ *(m=1–4)*: One difference between our calculations and experiment is that we used HCN as a ligand in place of CH_3CN for reasons of computational economy. HCN has a slightly higher binding energy than H_2O and, because CH_3CN is more basic than HCN, we expect that in complexes $[La(CH_3CN)_6(H_2O)_m]^{2+}$, for which $m>2$, the CH_3CN molecules will be in the first solvation shell, and that water molecules in the second shell will attach through hydrogen bonds to water molecules in the first shell. That is to say, we do not expect a change in the binding mode on substituting HCN for CH_3CN, and that the former will be a good and computationally less-expensive model for the latter ligand.

Firstly, we considered La^{3+} complexes in which HCN and H_2O molecules are directly attached to the metal ion, that is, all reside in the first coordination shell. For the complexes $[La(HCN)_n]^{3+}$ ($n=1$–6), only one structure was optimized for each n value, whereas for $[La(HCN)_6(H_2O)_m]^{3+}$ ($m=1$–4), several structures per m value were considered.

A square antiprism is the most common structure for $[La(HCN)_6(H_2O)_2]^{3+}$; this is a distorted cube with equivalent donor sites, but with reduced ligand–ligand repulsions. Four possible structures can be drawn by changing the relative sites of the two water molecule (Scheme 1)

During the structure optimizations, isomers **a** and **d** collapsed into isomers **c** and **b**, respectively, which have essentially the same energy (Figure 4 and Table 1).

The common geometries of nine-coordinate complexes are tricapped trigonal prismatic (D_{3d}) and monocapped square-antiprismatic (C_{4v}); however, interconversion between the two is relatively easy.[37] For $[La(HCN)_6(H_2O)_3]^{3+}$, starting with the tricapped trigonal prism structure, three water molecules are to be distributed between the three layers, and six possible geometries can be drawn (Scheme 2). The three digits in parentheses represent, respectively, the numbers of water molecules in the three layers, starting from the top.

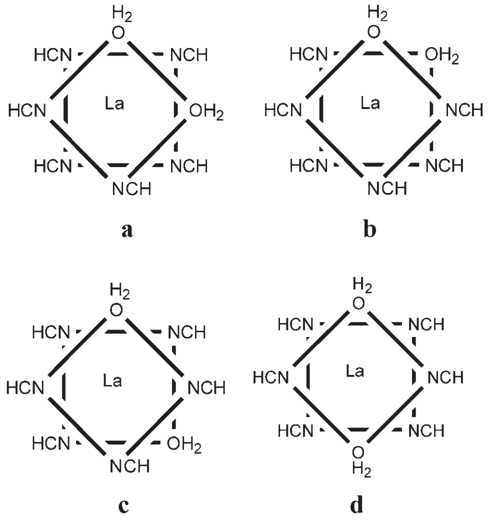

Scheme 1.

We first examined the geometries of isomers **c** and **d**, in which all three water molecules are located in the same layer. Calculations show isomer **c** to be only 0.1 kcal mol^{-1} higher in energy than isomer **d**. Next, we attempted to

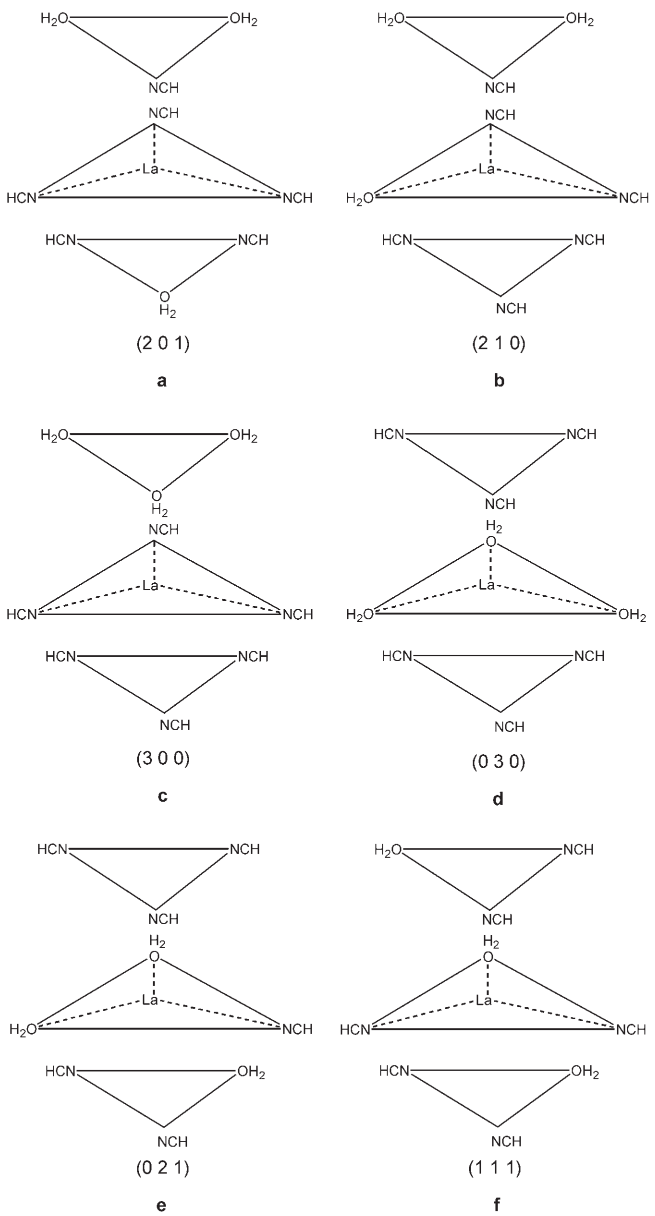

Scheme 2.

obtain an optimized structure for isomer **f**, which has one molecule of water in each layer. We found that the water molecule in the middle layer exchanges with an HCN in one of the outer layers, leading to isomer **a**. Again, the energy difference between isomers **a** and **d** is very small, only 0.1 kcal mol^{-1} at the B3LYP/sdd-f/6-31+G(d,p)//B3LYP/sdd-f/6-31G(d) level. These results indicate that the location of the different ligands in the tricapped trigonal prismatic structure has little effect on the energy.

If ten-fold coordination is assumed for complexes $[La(HCN)_6(H_2O)_4]^{3+}$, the bicapped square antiprism (D_{4d}) is expected to be the most stable.[37] Two isomers were optimized on the basis of this structure: one has two HCN molecules in the cap sites, $[La(HCN)_6(H_2O)_4]^{3+}{}_a$, and the other has two water molecules in the cap sites, $[La(HCN)_6(H_2O)_4]^{3+}{}_b$ (Figure 4). These structures have very similar energies: the one with the HCN molecules in the cap sites is lower by 0.3 kcal mol^{-1} (Table 1).

Complexes $[La(HCN)_{6-p}(H_2O)_m]^{3+}\cdot n(H_2O)p(HCN)$ *(*m+n=*1–4)*: Computational studies were carried out on a wide range of complexes of the form $[La(HCN)_{6-p}(H_2O)_m]^{3+}\cdot n(H_2O)p(HCN)$, with $(6-p)$HCN and mH$_2$O molecules in the first solvation shell, and nH$_2$O and pHCN molecules in the second shell and hydrogen bonded to molecules in the first shell. Because the ligand-binding energy of La^{3+} in $[La(HCN)]^{3+}$ is 15.1 kcal mol^{-1} higher than that in $[La(H_2O)]^{3+}$, the HCN molecules should occupy the first solvation shell. However, as the number of ligands increases, the sequential binding energy decreases monotonically and the difference in $\Delta H^{\circ}_{0(n,n-1)}$ between $[La(L)_{n-1}(HCN)]^{3+}$ and $[La(L)_{n-1}(H_2O)]^{3+}$ (L=HCN or H$_2$O) becomes smaller. Furthermore, because the water molecules provide protons that are more effective in hydrogen bonding, in some instances, a water molecule can displace an HCN molecule that resides in the first solvation shell. For example, $[La(HCN)_5(H_2O)_2]^{3+}\cdot HCN$ was found to be 0.6 kcal mol^{-1} lower in energy than $[La(HCN)_6(H_2O)]^{3+}\cdot H_2O$ at the B3LYP/sdd-f/6-31+G(d,p)//B3LYP/sdd-f/6-31G(d) level. As can be seen from Figure 4, the HCN molecule in the second solvation shell of $[La(HCN)_5(H_2O)_2]^{3+}\cdot HCN$ is bound to two water molecules in the first shell, forming a six-membered ring. By comparison, the water molecule in the second shell of $[La(HCN)_6(H_2O)]^{3+}\cdot H_2O$ can be hydrogen bonded to only one water molecule in the first shell. In complexes in which the number and strengths of hydrogen bonds to ligands in the second shell are similar, the HCN molecule always occupies the first solvation shell. At the B3LYP/sdd-f/6-31+G(d,p)//B3LYP/sdd-f/6-31G(d) level, the energy of $[La(HCN)_5(H_2O)_3]^{3+}\cdot HCN_b$ is 1.9 kcal mol^{-1} higher than that of $[La(HCN)_6(H_2O)_2]^{3+}\cdot H_2O$.

$[La(HCN)_6(H_2O)_2]^{3+}$: Two possible structures were optimized for $[La(L)_7]^{3+}\cdot L$ (L=HCN or H$_2$O). The energy of $[La(HCN)_5(H_2O)_2]^{3+}\cdot HCN$ is 0.6 kcal mol^{-1} lower than that of $[La(HCN)_6(H_2O)]^{3+}\cdot H_2O$ at the B3LYP/sdd-f/6-31+G(d,p)//B3LYP/sdd-f/6-31G(d) level. However, it is 1.5 kcal mol^{-1} higher in energy than the eight-coordinate structure in which all the ligands are directly coordinated to La^{3+} (Figure 4 and Table 1). Only one optimized structure was obtained for $[La(L)_6]^{3+}\cdot 2L$: the two molecules in the second solvation shell are both HCN molecules, and each is hydrogen bonded to a water molecule located in the first shell.

$[La(HCN)_6(H_2O)_3]^{3+}$: Three stable structures were obtained for $[La(L)_8]^{3+}\cdot L$ and these were all lower in energy (by more than 2.8 kcal mol^{-1}) than the structures in which all nine ligands were attached directly to La^{3+}. $[La(HCN)_6(H_2O)_2]^{3+}\cdot H_2O$ has the lowest energy: the water molecule in the second solvation shell is hydrogen bonded to both water molecules in the first shell, and all the HCN molecules are

in the first shell. One stable structure was located for $[La(L)_7]^{3+}\cdot 2L$. This has two HCN molecules in the second solvation shell, one bound to two water molecules and the other to the third water molecule in the first shell (see Figure 4). This structure is higher in energy than the eight-coordinate isomers by 3–5 kcal mol^{-1}.

$[La(HCN)_6(H_2O)_4]^{3+}$: Again, among the possible isomers, the eight-coordinate complexes have the lowest energies (Table 1). With respect to the lowest-energy isomer, $[La(HCN)_4(H_2O)_4]^{3+}\cdot 2HCN_b$, isomers with all ten ligands attached directly to the metal are ≈12 kcal mol^{-1} higher in energy and the nine-coordinate isomers are ≈3 kcal mol^{-1} higher in energy (Figure 4).

Energetics: La^{3+} first-shell binding energies: As the number of ligands increases, a significant amount of charge is transferred from La^{3+} to the ligands and the La–N(O) distances increase. As the number of ligands increases from 1 to 10, the Mulliken charge on La decreases monotonically from +2.64 to +1.42, and the La–N distance increases from 2.354 to 2.788 Å. This is accompanied by a decrease in the sequential binding energy for each successive ligand. The sequential binding energies and free energies in the *first* solvation shell of $[La(HCN)_6(H_2O)_m]^{3+}$ ($m=1$–4) are shown in Figure 5. As m increases from 0 to 1 (coordination number from six to seven), the decrease in binding energy at the B3LYP/sdd-f/6-31+G(d,p)//B3LYP/sdd-f/6-31G(d) level, labeled as ΔH^{o}_0(SG), is 10.0 kcal mol^{-1}; as it increases from 1 to 2 (coordination number from seven to eight), the decrease is 4.0 kcal mol^{-1}; as it increases from 2 to 3 (coordination number from eight to nine), the decrease is 5.6 kcal mol^{-1}; and as it increases from 3 to 4 (coordination number from nine to ten), the decrease is 6.6 kcal mol^{-1}. These results indicate that the sequential binding energy of the eighth ligand to La^{3+} is unusually large; similar trends are also evident in the other two plots that use the lower level of theory. These results support the conclusion drawn from the experimental results that La^{3+} prefers eight-coordination. Figure 6 summarizes the results for the various La complexes containing from eight to ten ligands.

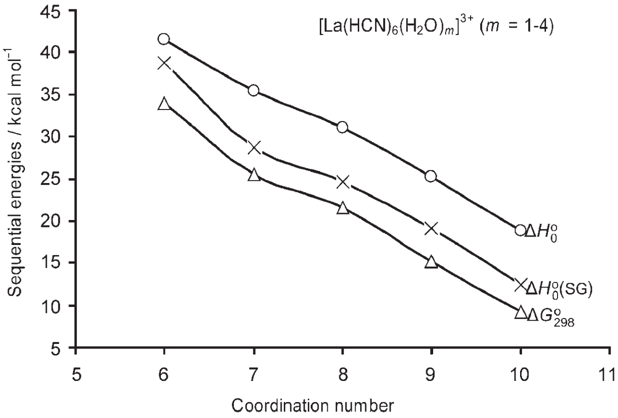

Figure 5. Sequential enthalpies $\Delta H^{o}_{n,n-1}$(0 K) and free energies $\Delta G^{o}_{n,n-1}$ (298 K) of stable $[La(HCN)_6(H_2O)_m]^{3+}$ ($m=1$–4). ΔH^{o}_0 andΔG^{o}_{298} were calculated at the B3LYP/sdd-f/6-31G(d) level, and ΔH^{o}_0(SG) was calculated at the B3LYP/sdd-f/6-31+G(d,p)//B3LYP/sdd-f/6-31G(d) level with a scaled zero-point energy (ZPE) correction.

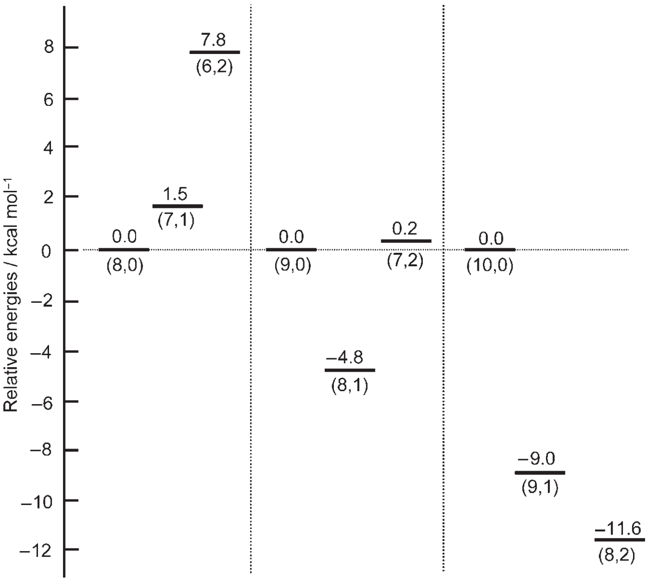

Figure 6. Energies for $[La(HCN)_{6-p}(H_2O)_{m-q}]^{3+}\cdot q(H_2O)p(HCN)$ ($6+m=$ 8–10) relative to complexes in which all ligands are directly connected to La^{3+}. The two numbers in parentheses are the numbers of ligands in the first and second solvation shells, respectively. Energies were calculated at the B3LYP/sdd-f/6-31+G(d,p)//B3LYP/sdd-f/6-31G(d) level with a scaled ZPE.

Comparison with solution results: How do our gas-phase results and conclusions compare to those obtained from solution studies? Wertz et al. used X-ray diffraction to obtain a coordination number of eight in experiments with various $LaCl_3$ solutions (0.6–2.7 M).[38] Habenschuss and Spedding used the same technique to investigate concentrated (>3 M) $LaCl_3$ solutions; they found a coordination number of nine.[39] Johansson et al. determined that a coordination number of eight best simulated their X-ray data recorded for 1–4.6 M perchlorate and selenate solutions of La^{3+}; however, using a coordination number of seven or nine did not decrease greatly the quality of their fits.[40] The most common coordination numbers for La^{3+} in solutions are eight and nine.[41] Examination of our calculated relative energies for $[La(HCN)_{6-p}(H_2O)_m]^{3+}\cdot n(H_2O)p(HCN)$ ($m+n=$ 1–4, Figure 6) reveals that the nine- and ten-ligand complexes with nine ligands in the primary solvation shell are only 4.8 and 2.6 kcal mol^{-1}, respectively, higher in energy than the complex with eight ligands in the primary shell and the remaining water molecules in the secondary shell. In addition, the seven-coordinate complex $[La(HCN)_5(H_2O)_2]^{3+}\cdot HCN$ is only 1.5 kcal mol^{-1} higher in energy than the eight-coordinate complex $[La(HCN)_6(H_2O)_2]^{3+}{}_c$. Thus, the energy differences among the complexes are sufficiently small for seven-, eight-, and nine-coordination to be plausible, and, thus, they may exist in the gas phase. This flexibility is in accordance with lanthanum's solution chemistry.

Conclusion

Literature data for Ca^{2+} give a coordination number of six, a fact confirmed by our experimental and computational work. This verifies the utility and performance of our approach. The examination of a series of La complexes indicates that the preferred direct coordination number of La^{3+} is eight, with the eight ligands arranged in a square-antiprism geometry. Additional ligands are accommodated in the second solvation shell and are hydrogen bonded to one or (better) two water molecules in the first solvation shell.

Acknowledgements

This study was supported by the Natural Sciences and Engineering Research Council (NSERC) of Canada, MDS SCIEX, and York University.

---

[1] Y. Marcus, *Ion Solvation*, Wiley, New York, **1985**.
[2] P. Kebarle, *Annu. Rev. Phys. Chem.* **1977**, *28*, 445.
[3] R. G. Keesee, A. W. Castleman, Jr., *J. Phys. Chem. Ref. Data* **1986**, *15*, 1011.
[4] P. Kebarle, *Modern Aspects of Electrochemistry* (Eds.: B. E. Conway, J. O'M. Bockris), Plenum Press, New York, **1974**, Vol. 9, p. 1.
[5] A. W. Castleman, Jr., K. H. Bowen, Jr., *J. Phys. Chem.* **1996**, *100*, 12911, and references therein.
[6] A. J. Stace, *J. Phys. Chem. A* **2002**, *106*, 7993.
[7] a) M. Peschke, A. T. Blades, P. Kebarle, *J. Phys. Chem. A* **1998**, *102*, 9978; b) M. Peschke, A. T. Blades, P. Kebarle, *J. Am. Chem. Soc.* **2000**, *122*, 10440; c) M. Peschke, A. T. Blades, P. Kebarle, *J. Am. Chem. Soc.* **2000**, *122*, 1492.
[8] a) S. E. Rodriguez-Cruz, R. A. Jockusch, E. R. Williams, *J. Am. Chem. Soc.* **1998**, *120*, 5842; b) S. E. Rodriguez-Cruz, R. A. Jockusch, E. R. Williams, *J. Am. Chem. Soc.* **1999**, *121*, 1986; c) S. E. Rodriguez-Cruz, R. A. Jockusch, E. R. Williams, *J. Am. Chem. Soc.* **1999**, *121*, 8898; d) R. L. Wong, E. R. Williams, *Int. J. Mass Spectrom.* **2004**, *232*, 59.
[9] G. Vitale, A. B. Valina, H. Huang, R. Amunugama, M. T. Rodgers, *J. Phys. Chem. A* **2001**, *105*, 11351.
[10] a) C. W. Bock, J. P. Glusker, *Inorg, Inorg. Chem.* **1993**, *32*, 1242; b) C. W. Bock, A. Kaufman, J. P. Glusker, *Inorg. Chem.* **1994**, *33*, 419; c) C. W. Bock, A. K. Katz, J. P. Glusker, *J. Am. Chem. Soc.* **1995**, *117*, 3754; d) A. K. Katz, J. P. Glusker, S. A. Beebe, C. W. Bock, *J. Am. Chem. Soc.* **1996**, *118*, 5752.
[11] E. D. Glendening, D. Feller, *J. Phys. Chem.* **1996**, *100*, 4790.
[12] M. Pavlov, P. E. M. Siegbahn, M. Sandström, *J. Phys. Chem. A* **1998**, *102*, 219.
[13] D. Asthagiri, L. R. Pratt, M. E. Paulaitis, S. B. Rempe, *J. Am. Chem. Soc.* **2004**, *126*, 1285.
[14] a) A. T. Blades, P. Jayaweera, M. G. Ikonomou, P. Kebarle, *Int. J. Mass Spectrom. Ion Process* **1990**, *101*, 325; b) A. T. Blades, P. Jayaweera, M. G. Ikonomou, P. Kebarle, *Int. J. Mass. Spectrom. Ion Process* **1990**, *102*, 251; c) P. Jayaweera, A. T. Blades, M. G. Ikonomou, P. Kebarle, *J. Am. Chem. Soc.* **1990**, *112*, 2452.
[15] a) Z. L. Cheng, K. W. M. Siu, R. Guevremont, S. S. Berman, *J. Am. Soc. Mass Spectrom.* **1992**, *3*, 281; b) Z. L. Cheng, K. W. M. Siu, R. Guevremont, S. S. Berman, *Org. Mass Spectrom.* **1992**, *27*, 1370; c) A. A. Shvartsburg, K. W. M. Siu, *J. Am. Chem. Soc.* **2001**, *123*, 10071; d) A. A. Shvartsburg, J. G. Wilkes, J. O. Lay, K. W. M. Siu, *Chem. Phys. Lett.* **2001**, *350*, 216.
[16] a) A. A. Shvartsburg, *J. Am. Chem. Soc.* ***2002**, 124*, 7910; b) A. A. Shvartsburg, *J. Am. Chem. Soc.* **2002**, *124*, 12343; c) A. A. Shvartsburg, *Chem. Phys. Lett.* **2002**, *360*, 479.
[17] a) C. Seto, J. A. Stone, *Int. J. Mass Spectrom. Ion Processes* **1998**, *175*, 263; b) J. A. Stone, D. Vukomanovic, *Int. J. Mass Spectrom.* **1999**, *185–187*, 227; c) D. Vukomanovic, J. A. Stone, *Int. J. Mass Spectrom.* **2000**, *202*, 251; d) J. A. Stone, D. Vukomanovic, *Chem. Phys. Lett.* **2001**, *346*, 419.
[18] P. Vitorge, M. Masella, *Chem. Phys. Lett.* **2000**, *332*, 367.
[19] H. Cox, G. Akibo-Betts, R. R. Wright, N. R. Walker, S. Curtis, B. Duncombe, A. J. Stace, *J. Am. Chem. Soc.* **2003**, *125*, 233.
[20] N. R. Walker, R. R. Wright, A. J. Stace, C. A. Woodward, *Int. J. Mass Spectrom.* **1999**, *188*, 113.
[21] M. F. Bush, R. J. Saykally, E. R. Williams, *Int. J. Mass Spectrom.* **2006**, *253*, 256.
[22] D. R. Lide, *CRC Handbook of Chemistry and Physics*, 84th ed., CRC Press, p. 10–178.
[23] a) R. N. Grewal, H. El Aribi, A. G. Harrison, K. W. M. Siu, A. C. Hopkinson, *J. Phys. Chem. B* **2004**, *108*, 4899; b) H. El Aribi, G. Orlova, A. C. Hopkinson, K. W. M. Siu, *J. Phys. Chem. A* **2004**, *108*, 3844; c) T. Shi, J. Zhao, T. Shoeib, K. W. M. Siu, A. C. Hopkinson, *Eur. J. Mass Spectrom.* **2004**, *10*, 931.
[24] a) N. G. Tsierkezos, D. Schröder, H. Schwarz, *J. Phys. Chem. A* **2003**, *107*, 9575; b) N. G. Tsierkezos, D. Schröder, H. Schwarz, *Int. J. Mass Spectrom.* **2004**, *235*, 33.
[25] N. F. Dalleska, K. Honma, L. S. Sunderlin, P. B. Armentrout, *J. Am. Chem. Soc.* **1994**, *116*, 3519.
[26] a) T. Shoeib, H. El Aribi, K. W. M. Siu, A. C. Hopkinson, *J. Phys. Chem. A* **2001**, *105*, 710; b) H. El Aribi, C. F. Rodriquez, D. R. P. Almeida, Y. Ling, W. W.-N. Mak, A. C. Hopkinson, K. W. M. Siu, *J. Am. Chem. Soc.* **2003**, *125*, 9229.
[27] P. A. Steiner, W. Gordy, *J. Mol. Spectrosc.* **1966**, *21*, 291.
[28] T. Shi, G. Orlova, J. Guo, D. K. Bohme, A. C. Hopkinson, K. W. M. Siu, *J. Am. Chem. Soc.* **2004**, *126*, 7975.
[29] T. Shi, J. Zhao, A. C. Hopkinson, K. W. M. Siu, *J. Phys. Chem. B* **2005**, *109*, 10590.
[30] Gaussian 98 (Revision A 11): M. J. Frisch, G. W. Trucks, H. B. Schlegel, G. E. Scuseria, M. A. Robb, J. R. Cheeseman, V. G. Zakrzewski, J. A. Montgomery, Jr., R. E. Stratmann, J. C. Burant, S. Dapprich, J. M. Millam, A. D. Daniels, K. N. Kudin, M. C. Strain, O. Farkas, J. Tomasi, V. Barone, M. Cossi, R. Cammi, B. Mennucci, C. Pomelli, C. Adamo, S. Clifford, J. Ochterski, G. A. Petersson, P. Y. Ayala, Q. Cui, K. Morokuma, D. K. Malick, A. D. Rabuck, K. Raghavachari, J. B. Foresman, J. Cioslowski, J. V. Ortiz, B. B. Stefanov, G. Liu, A. Liashenko, P. Piskorz, I. Komaromi, R. Gomperts, R. L. Martin, D. J. Fox, T. A. Keith, M. A. Al-Laham, C. Y. Peng, A. Nanayakkara, C. Gonzales, M. Challacombe, P. M. W. Gill, B. G. Johnson, W. Chen, M. W. Wong, J. L. Andres, C. Gonzales, M. Head-Gordon, E. S. Replogle, J. A. Pople, Gaussian Inc., Pittsburgh, PA, **2001**.
[31] A. D. Becke, *Phys. Rev. A* **1988**, *38*, 3098.
[32] A. D. Becke, *J. Chem. Phys.* **1993**, *98*, 5648.
[33] C. Lee, W. Yang, R. G. Parr, *Phys. Rev. B* **1988**, *37*, 785.
[34] M. Dolg, H. Stoll, A. Sovin, H. Preuss, *Theor. Chim. Acta* **1989**, *75*, 173.
[35] D. Schröder, H. Schwarz, J. N. Harvey, *J. Phys. Chem. A* **2000**, *104*, 11257.
[36] J. B. Foresman, A. Frisch, *Exploring Chemistry with Electronic Structure Methods*, 2nd ed., Gaussian, Pittsburgh PA, **1996**.
[37] M. G. B. Drew, *Coord. Chem. Rev.* **1977**, *24*, 179.
[38] a) L. S. Smith, D. L. Wertz, *J. Am. Chem. Soc.* **1975**, *97*, 2365; b) M. L. Steele, D. L. Wertz, *Inorg. Chem.* **1977**, *16*, 1225.
[39] A. Habenschuss, F. H. Spedding, *J. Chem. Phys.* **1979**, *70*, 2797.
[40] G. Johansson, H. Wakita, *Inorg. Chem.* **1985**, *24*, 3047.
[41] F. A. Cotton, G. Wilkindson, *Advanced Inorganic Chemistry*, 6th ed., Wiley, New York, **1999**.

Received: July 24, 2006